Supporting Information

Inter-helix distances in lysophospholipid micelle-bound alpha-synuclein from pulsed ESR measurements

Peter Borbat,[†] Trudy F. Ramlall,[‡] Jack H. Freed,[†] and David Eliezer*[‡]

[†]Department of Chemistry and Biochemistry, Cornell University, Ithaca, NY 14853, and

[‡]Department of Biochemistry and Program in Structural Biology, Weill Medical College of Cornell University, 1300 York Avenue, New York, NY 10021

Further Experimental Details:

DEER experiments were conducted at the working frequency of 17.4 GHz in the Ku band on a modified pulsed ESR spectrometer (Ref. 7 of main text). A second TWT amplifier and independent pulse forming channels were added. The output pulse of the second TWTA has been combined with the main pulse output using a directional coupler. 4-pulse DEER has been used in all cases shown with pulse widths of 16/32/32 ns in the detection mode and 32 ns in the pump mode, respectively. The frequency separation between the two modes was set at 65 MHz with the pump pulse applied at the center peak of the ESR spectrum.the

The time domain DEER signals and the extracted inter-nitroxide distances for all 13 double mutants studied are shown in Figures S1 to S12 and Tables S1 and S2 below. Note that maxima are offset from average distance in few cases and that the flexibility of nitroxide side-chain adds to width of the distance distribution originating from the conformational space of the protein itself. However the effect on average distances in this range is usually small to moderate and the distances between nitroxides have been shown to correlate with Cα-Cα distances (ref 6c in main text and ref SM1 below).

To evaluate the possibility of inter-molecular contributions to our distance measurements we performed experiments using singly spin-labeled αS (labeled at position S42). Data from this single mutant (not shown) fall onto a straight line in a log plot vs. time with a slope that is consistent with a uniform spin distribution corresponding to the protein concentration used in this control experiment (100 μM). This indicates that the concentration of any oligomeric protein fraction was below the detection limit. In addition, the good agreement between the measured and expected distances in the H50C/T72C control sample argues strongly against any contribution from inter-molecular distances. This is as expected, because we were careful to work at protein concentrations which were significantly lower than the micelle concentrations (estimated based on aggregation numbers of ~60 for SDS and ~120 for LPPG), effectively limiting the number of protein molecules per micelle to one. Also notably, at the protein to detergent ratio used here, previous NMR and ultracentrifugation data confirmed that the protein remains monomeric.

Our choice of LPPG as an alternative to SDS was guided by the fact that LPPG is an authentic phospholipids with a biologically relevant headgroup, is not considered a protein denaturant, and has been shown to be effective in maintaining membrane protein structure (ref SM2). A negatively charged headgroup was chosen because αS exhibits a strong preference for anionic lipids, binding only weakly to zwitterionic headgroups (refs SM3 and SM4). The C-terminal tail of αS is highly negatively charged (net charge for residues 103-140 of -14), and does not contribute to the lipid binding of the protein, which is mediated entirely by the positively charged N-terminal lipid-binding domain (net charge of residues 1-102 of +5). The sequence of the full length protein, with charged residues highlighted, is shown in Figure S13 below.

References:

SM1. Sale, K.; Song, L. K.; Liu, Y. S.; Perozo E.; Fajer, P. *J Am Chem Soc* **2005**, *127*, 9334-9335.

SM2. Krueger-Koplin, R. D.; Sorgen, P. L.; Krueger-Koplin, S. T.; Rivera-Torres, I. O.; Cahill, S. M.; Hicks, D. B.; Grinius, L.; Krulwich, T. A.; Girvin, M. E. *J Biomol NMR*, **2004**, *28*, 43-57.

SM3. Bussell, R. Jr.; Eliezer, D. *Biochemistry*, **2004**, *43*, 4810-4818.

SM4. Rhoades, E.; Ramlall, T. F.; Webb, W. W.; Eliezer, D. **2006**, *90*, 4692-4700.

Figures S1-S12: Time domain DEER signals, with the background removed by subtraction of the linear part of decay in log plots, and respective distance distributions produced by Tikhonov regularization as described in Ref. 8 of main text. Data for LPPG are shown in blue and for SDS in red.

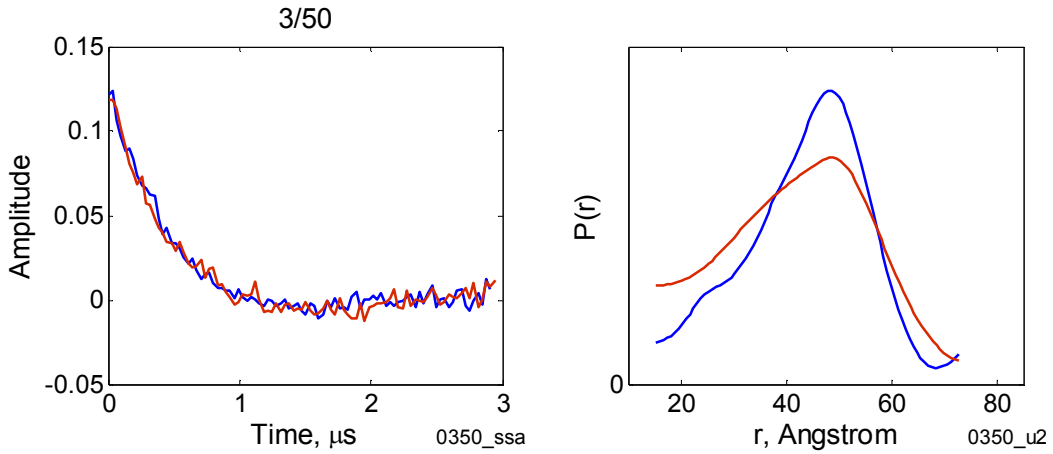

Figure S1.

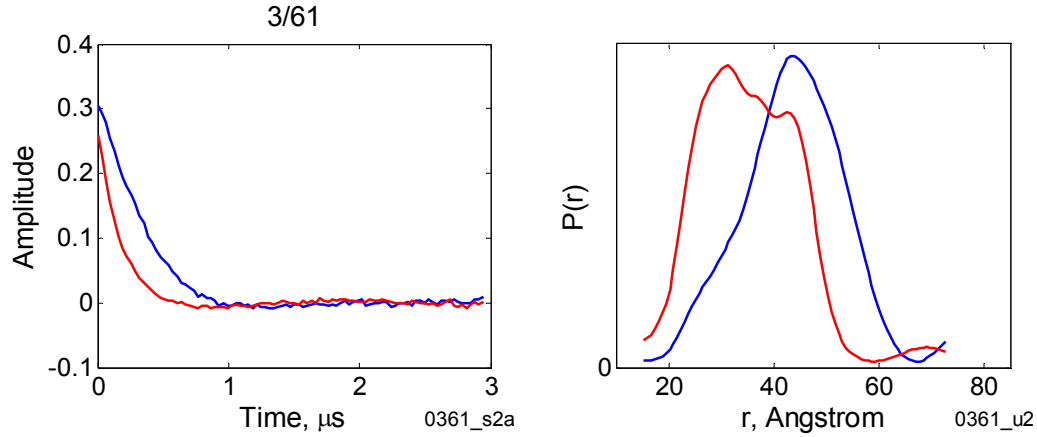

Figure S2.

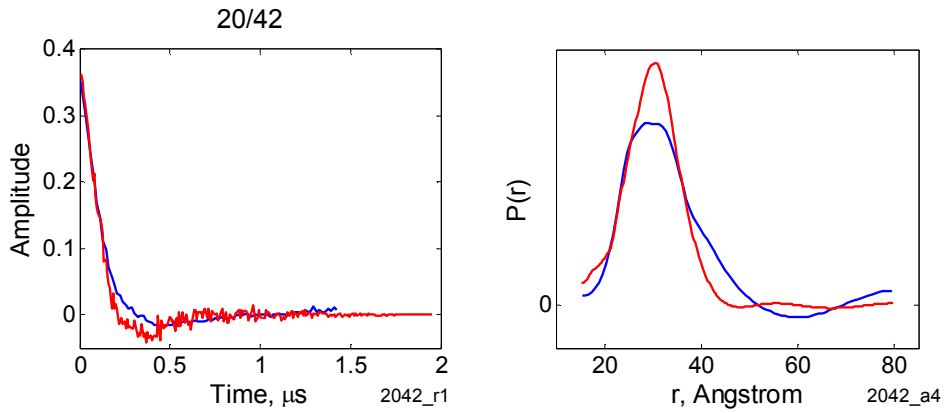

Figure S3.

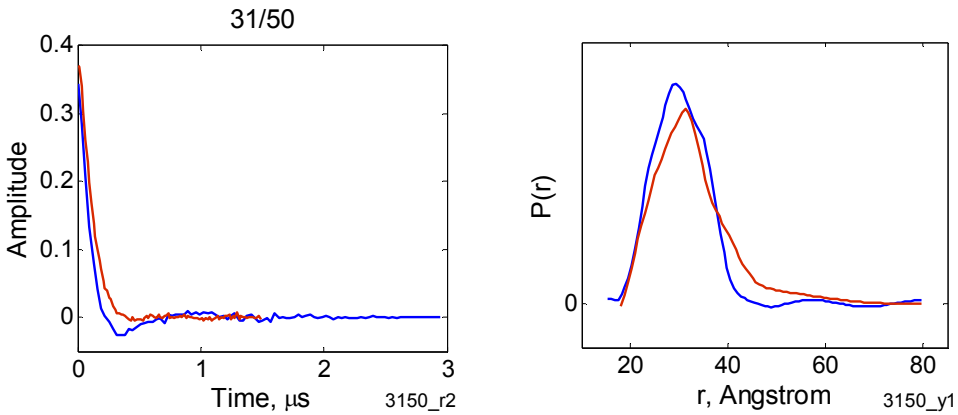

Figure S4.

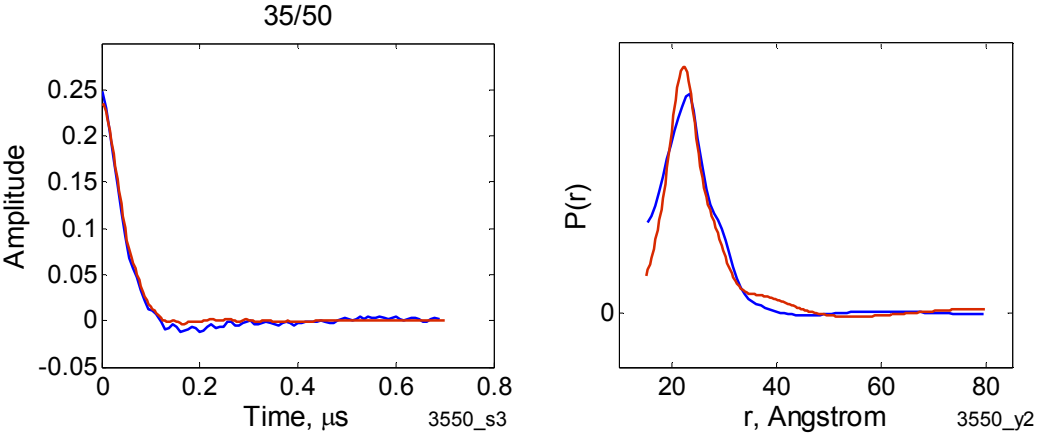

Figure S5.

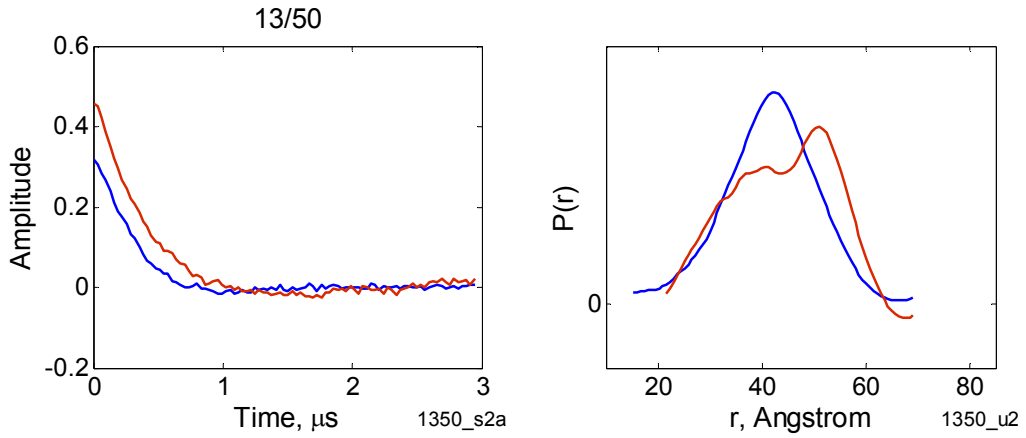

Figure S6.

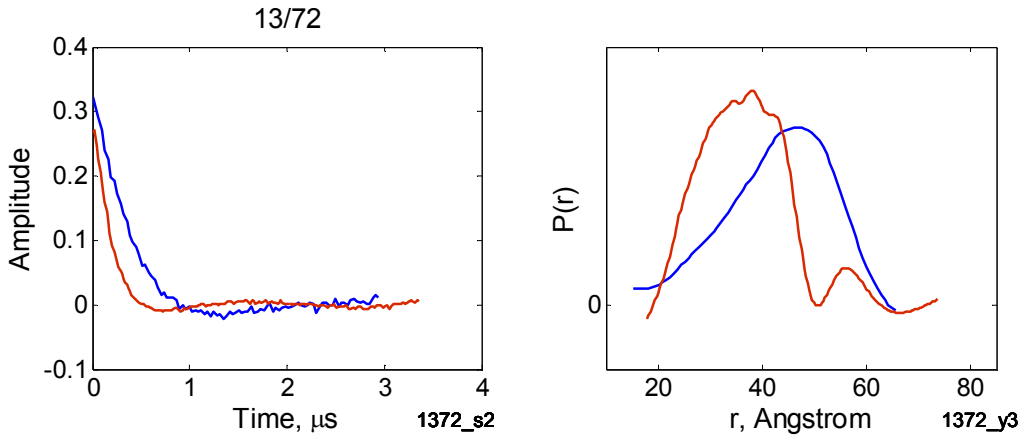

Figure S7.

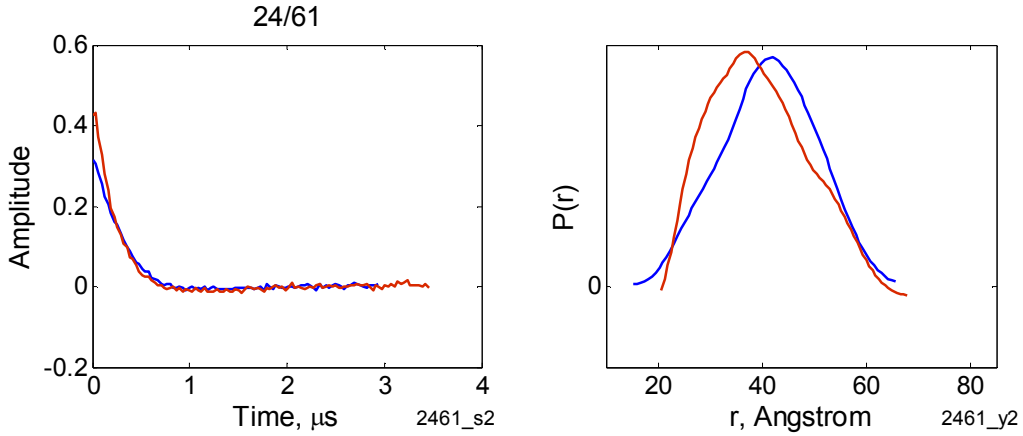

Figure S8.

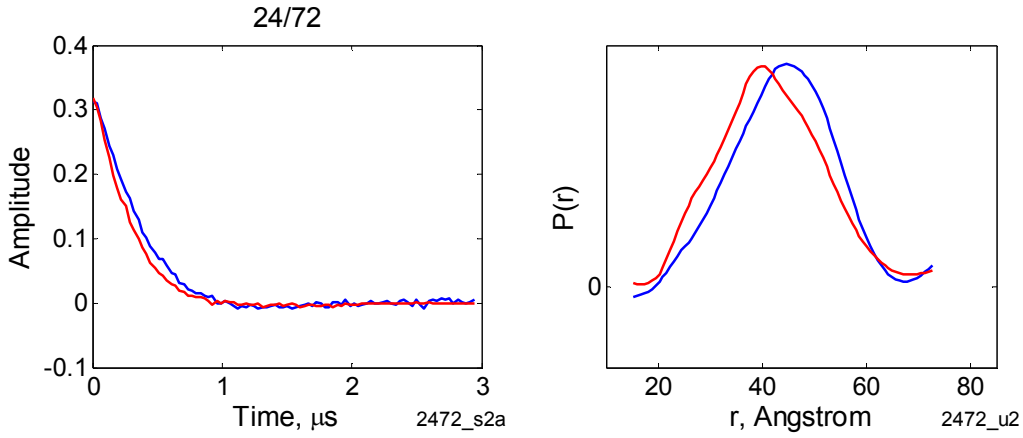

Figure S9.

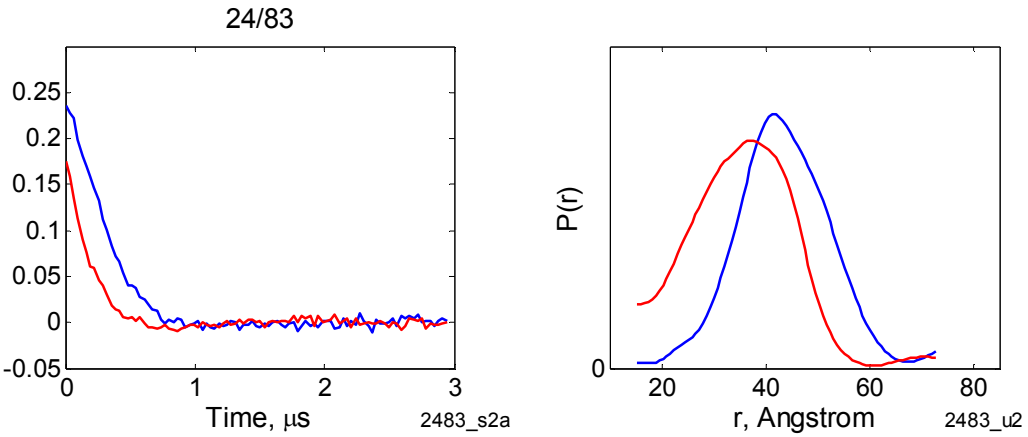

Figure S10.

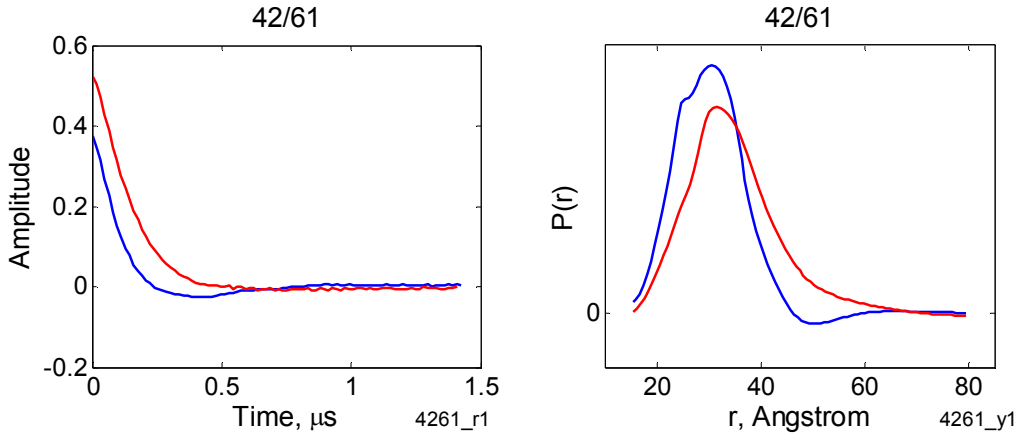

Figure S11.

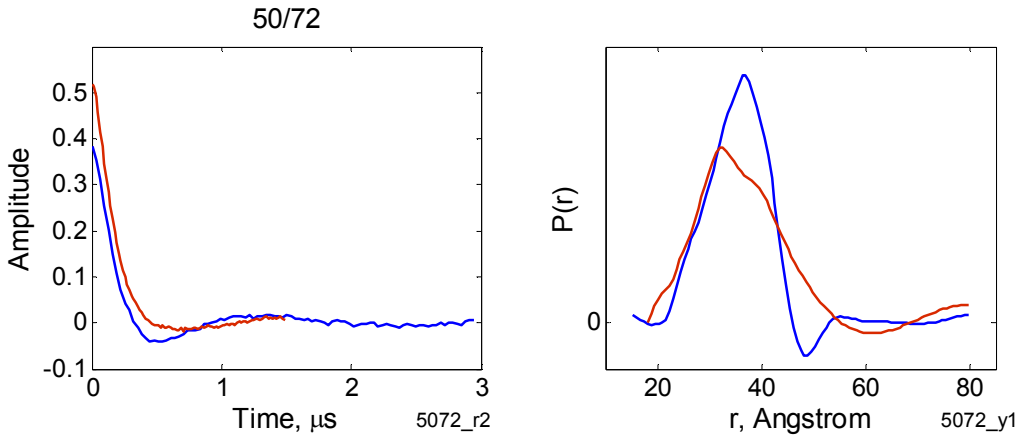

Figure S12.

Figures S13: Amino acid sequence of full length human αS. Lysines are highlighted in cyan and aspartates and glutamates in red.

```
1           11          21          31          41          51          61
↓           ↓           ↓           ↓           ↓           ↓           ↓
MDVFMKGLSK AKEGVVAAAE KTKQGVAEAA GKTKEGVLYV GSKTKEGVVH GVATVAEKTK EQVTNVGGAV

VTGVTAVAQK TVEGAGSIAA ATGFVKKDQL GKNEEGAPQE GILEDMPVDP DNEAYEMPSE EGYQDYEPEA
↑           ↑           ↑           ↑           ↑           ↑           ↑
71          81          91          101         111         121         131
```

Tables:

Table S1: Distances between nitroxide spin-labels in α-Synuclein in LPPG.

Mutant	R_{av}, Å	$\sqrt{\langle (r - R_{av})^2 \rangle}$, Å	Maximum, Å
H50C/T72C[(b)].	35	6.1	37.7
E35C/H50C[(a)].	23.8	5.1	24.3
Q24C/E61C[(a)].	42.6	11	42.6
E13C/T72C[(a)].	44	11	47.5
V3C/E83C[(a)].	34.6	10.5	29.3 & 34
Q24C/T72C[(a)].	46	9.7	49.6
Q24C/E83C[(a)].	43.5	9.6	42
V3C/E61C[(a)].	44.8	11.4	44.7
V3C/H50C[(a)].	45	13	49.2
E13C/H50C[(a)].	42.7	10.5	43.3
G31C/H50C[(b)].	30.2	5.7	30
E20C/S42C[(b)].	31.6	8	29.8
S42C/E61C[(b)].	29.8	6.1	31.2

(a) – Full-length
(b) – 103 stop

Table S2: Distances between nitroxide spin-labels in α-Synuclein in SDS.

Mutant	R_{av}, Å	$\sqrt{\langle (r - R_{av})^2 \rangle}$, Å	R_{max}, Å
H50C/T72C[(b)].	36	9.4	33.3
E35C/H50C[(b)].	24.7	7.3	28.5
Q24C/E61C[(b)].	40.5	9	37
E13C/T72C[(b)].	37	9.3	38.2
V3C/E83C[(b)].	28.1	7.9	26.3
Q24C/T72C[(a)].	42.7	11.4	40.5
Q24C/E83C[(a)].	36.1	10.4	37.7
V3C/E61C[(a)].	36	10.2	32 & 43
V3C/H50C[(a)].	43	15.3	48.9
E13C/H50C[(a)].	45	11.3	39 & 51.7
G31C/H50C[(b)].	32.8	8.2	31.9
E20C/S42C[(b)].	30	5.0	31
S42C/E61C[(b)].	34.4	8.5	32.1

(a) – Full-length
(b) – 103 stop